

# Large index-fingertip forces are produced by subject-independent patterns of muscle excitation

Francisco J. Valero-Cuevas<sup>a, b, \*</sup>, Felix E. Zajac<sup>a, b, c</sup>, Charles G. Burgar<sup>a, d</sup>

<sup>a</sup> Rehabilitation Research and Development Center, Veterans Affairs Palo Alto Health Care System, Palo Alto, CA 94304-1200, U.S.A.

<sup>b</sup> Mechanical Engineering Department, Biomechanical Engineering Division, Stanford University, Stanford, CA 94305-3030, U.S.A.

<sup>c</sup> Department of Functional Restoration, Stanford University, Stanford, CA, U.S.A.

<sup>d</sup> Physical Medicine and Rehabilitation, Stanford University, Stanford, CA, U.S.A.

Received in final form 27 May 1998

## Abstract

Are fingertip forces produced by subject-independent patterns of muscle excitation? If so, understanding the mechanical basis underlying these muscle coordination strategies would greatly assist surgeons in evaluating options for restoring grasping. With the finger in neutral ad- abduction and flexed 45° at the MCP and PIP, and 10° at DIP joints, eight subjects attempted to produce maximal voluntary forces in four orthogonal directions perpendicular to the distal phalanx (palmar, dorsal, lateral and medial) and in one direction collinear with it (distal). Forces were directed within  $4.7 \pm 2.2^\circ$  (mean  $\pm$  S.D.) of target and their magnitudes clustered into three distinct levels ( $p < 0.05$ ; post hoc pairwise RMANOVA). Palmar ( $27.9 \pm 4.1$  N), distal ( $24.3 \pm 8.3$  N) and medial ( $22.9 \pm 7.8$  N) forces were highest, lateral ( $14.7 \pm 4.8$  N) was intermediate, and dorsal ( $7.5 \pm 1.5$  N) was lowest. Normalized fine-wire EMGs from all seven muscles revealed distinct muscle excitation groups for palmar, dorsal and distal forces ( $p < 0.05$ ; post hoc pairwise RMANOVA). Palmar force used flexors, extensors and dorsal interosseous; dorsal force used all muscles; distal force used all muscles except for extensors; medial and lateral forces used all muscles including significant co-excitation of interossei. The excitation strategies predicted to achieve maximal force by a 3-D computer model (four pin joints, inextensible tendons, extensor mechanism and isometric force models for all seven muscles) reproduced the observed use of extensors and absence of palmar *interosseous* to produce palmar force (to regulate net joint flexion torques), the absence of extensors for distal force, and the use of intrinsics (strong MCP flexors) for dorsal force. The model could not predict the interossei co-excitation seen for medial and lateral forces, which may be a strategy to prevent MCP joint damage. The model predicts distal force to be most sensitive to dorsal interosseous strength, and palmar and distal forces to be very sensitive to MCP and PIP flexor moment arms, and dorsal force to be sensitive to the moment arm of and the tension allocation to the PIP extensor tendon of the extensor mechanism. © 1998 Elsevier Science Ltd. All rights reserved.

**Keywords:** Hand; Finger; Grasping; Biomechanical model; Muscle coordination; Electromyography; Maximum voluntary contraction; EMG

## 1. Introduction

The functional outcome of surgeries to restore grasping can vary depending on patient selection, available musculature, surgical technique, and rehabilitation (Hentz, et al., 1988, 1992; McFarlane, 1987). Because individuals can learn to coordinate the modified actions of hand muscles following tendon transfer surgeries

(Leffert and Meister, 1976; Moberg, 1990; Waters et al., 1990), musculoskeletal rather than neural factors seem to affect grasping outcomes most. Functional grasping requires well-directed fingertip forces of sufficient magnitude (Murray et al., 1994), and understanding the mechanical basis underlying the coordination of index-finger muscles would greatly assist surgeons in evaluating options for restoring grasping.

Published intramuscular electromyograms (EMGs) recorded during index-finger force production (Close and Kidd, 1969; Long et al., 1970; Maier and Hepp-Reymond, 1995) do not provide a consistent foundation from which to study muscle coordination during static

\* Corresponding author. Address: Mechanical Engineering Department, Biomechanical Engineering Division, Stanford University, Stanford, CA 94305-3030, U.S.A. Tel.: 650 493 5000; fax: 650 493 4919; e-mail: valero@roses.stanford.edu

grasping. No study has simultaneously recorded EMGs from all seven index-finger muscles during maximal finger force production. Because the index-finger has three flexion mechanical degrees of freedom (DOFs), the distal phalanx can impart a torque in the sagittal plane to an object in contact with it (i.e., distal phalanx torque) independently of the fingertip force it can transmit. Previous force measurement techniques may confound the interpretation of EMGs because the compliant and high-friction interface between the finger pad and dynamometer allow production of distal phalanx torque, which is not measured, and latitude in the direction of force application. Lastly, finger (Mathiowetz et al., 1985; Weightman and Amis, 1982) and wrist (O'Driscoll et al., 1992) posture affects finger mechanics and muscle fiber length, which influence muscle force and EMG output (Zajac, 1992). Such factors may explain the inconsistency in reported maximal tip and key pinch forces (19–106 N (An et al., 1985; Weightman and Amis, 1982)) and EMG patterns (Close and Kidd, 1969; Long et al., 1970; Maier and Hepp-Reymond, 1995).

Index-finger computer models are limited in their ability to explore the functional role of individual anatomical structures during production of well-directed fingertip forces. Models have either reduced the number of independent muscles (Weightman and Amis, 1982) or set some muscle forces to zero (An et al., 1979, 1985; Harding et al., 1993; Weightman and Amis, 1982). Sagittal plane models (Harding et al., 1993; Lee and Rim, 1990; Spoor, 1983; Weightman and Amis, 1982) cannot be used to study either laterally directed forces (as in key pinch) or muscle coordination necessary to retain the finger neutrally abducted during sagittal-plane force generation. Conversely, complex models are generally statically indeterminate and cause ambiguity in the muscle excitation pattern producing a given finger force (Chao and An, 1978). Nevertheless, unique excitation patterns are predicted to achieve maximal finger forces, regardless of the complexity of the system (Chao and An, 1978; Gordon, 1990; Kuo and Zajac, 1993; Spoor, 1983). The computational demands of geometric methods have precluded their application to finger models with more than one degree of static indeterminacy.

Fingertip forces unaccompanied by distal phalanx torque are applicable to prehension because they are necessary to grasp small or smooth (slippery) objects without the fingertip rotating or slipping, as well as to the prehension of large or rough objects (Murray et al., 1994). We hypothesize that isometric, well-defined fingertip force during a maximal voluntary contraction in a specific finger posture is produced by an excitation pattern that is statistically the same across subjects (i.e., subject-independent), and a 3D seven-muscle computer model would provide a mechanical basis for the patterns observed.

## 2. Materials and methods

Eight subjects ( $27 \pm 6$  (S.D.) yr) produced static force in five randomized directions (palmar, distal, lateral, dorsal and medial) against a rigidly held three-axis force sensing plate with the index-finger of their right-dominant hand (Fig. 1). The standardized flexed posture put the finger joints away from their extremes of range of motion and made active muscle forces, not passive muscle or joint structures, the principal contributors to fingertip force. Subjects wore a thimble molded to the contour of their distal phalanx with 5 mm metal balls embedded in locations corresponding to each force direction. The low-friction point contact defined by each ball against the force sensing surface required subjects to (i) accurately direct forces (otherwise the thimble would slip) and (ii) refrain from producing a distal phalanx torque

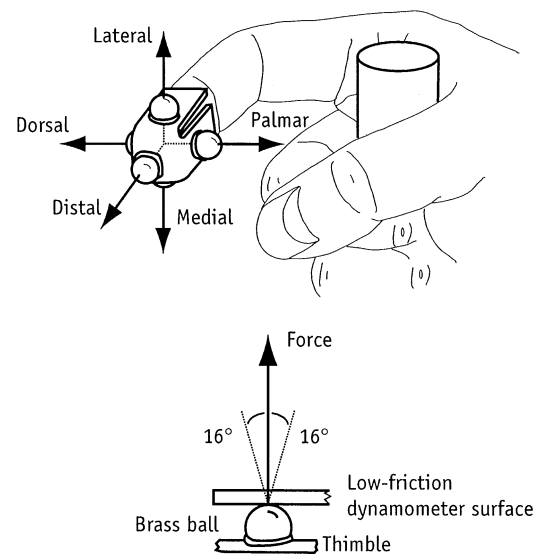


Fig. 1. Production of well-directed finger tip forces. Subjects placed their forearm in a trough, wrapped their dominant right hand around a fixed dowel to isolate index finger function and generated three maximal index finger forces in the dorsal, palmar, distal, lateral and medial directions in randomized order while maintaining a standard posture (finger in neutral ad-abduction,  $45^\circ$  flexion at metacarpophalangeal (MCP) and proximal interphalangeal (PIP) joints, and  $10^\circ$  flexion at distal interphalangeal (DIP) joint; wrist in full extension and neutral radial deviation; index not resting against middle finger). Subjects wore custom thimbles (thermoplastic splinting material, North Coast Medical, Inc.) with 5 mm brass balls that defined the directions of force production. A three-axis dynamometer (0.1 N resolution in all axes) was positioned and rigidly held by a 6-DOF Stäubli-Unimate Puma 260 robot arm (not shown) such that one ball at a time came in contact with the low-friction surface of the dynamometer. The friction characteristics of the contact required finger force to be directed within  $16^\circ$  of the surface normal for the ball in contact not to slip. Distal phalanx torque had to be zero for the thimble not to rotate about the contact point. Palmar and distal forces are applicable to 'tip pinch' and lateral force to 'key pinch,' two grasping modalities often targeted for surgical restoration (McFarlane, 1987; Hentz et al., 1988, 1992).

(otherwise the thimble would rotate about the point of contact). A programmable robotic arm accurately and quickly positioned the force sensing plate in contact with each metal ball (Valero-Cuevas, 1997).

We instructed subjects to increase force magnitude (a trace on a computer screen) beyond the previous maximum (a reference line on the screen) while maintaining finger posture. We collected three trials per direction after a preliminary trial provided the starting maximum. Visual feedback was included to help improve performance (Graves and James, 1990). Fiducial markers on the medial aspects of the finger were monitored on video to repeatably achieve the flexed posture. Video recordings during force production showed no apparent movement of fiducial markers, indicating subjects maintained the posture. The few (< 5%) cases in which the thimble slipped or rotated were repeated. Sufficient time between trials (at least 30 s) prevented fatigue (Enoka and Stuart, 1992). In a second randomized session the following day, we simultaneously recorded muscle activity using fine-wire electrodes placed in the seven muscles of the index-finger (Burgar et al., 1997) (Fig. 2). EMG signals were normalized to the largest of the maximal isometric voluntary contractions (MVC) recorded for each muscle in the same posture immediately before and after force production. Prior to participation, subjects read and signed a consent form approved by the Medical Committee for Protection of Human Subjects in Research at Stanford University.

The trial with the largest peak force per direction was analyzed. Average maximal force and muscle excitation levels were calculated from a 750 ms window centered on peak force (Fig. 2). Repeated-measures ANOVA tested for subject-independent differences in force magnitudes across sessions and directions, and for subject-independent differences in EMG levels across muscles for each direction. When a significant effect was found for any factor, post hoc pairwise comparisons tested for significant groupings of force magnitudes or muscle excitation levels.

The nominal computer model contains a fixed metacarpal and three phalanges articulated by four DOFs (Fig. 3A) and driven by seven independent muscles. The torques each muscle produced at all joints spanned by its tendon (i.e., joint torque vector) were calculated based on moment arms measured from a single fresh cadaver (An et al., 1983) and a radio-ulnarly symmetric extensor mechanism (Fig. 4). The extensor mechanism model was based on Winslow's tendinous rhombus (Zancolli, 1979) (Fig. 4A) and defined the distribution of EIP, EDC, PI and LUM forces at the interphalangeal joints. The lateral portions were implemented as a 'floating net' where vector distribution results in the algebraic sum of tensions in the diagonal and lateral bands exceeding the input PI and LUM forces simply due to their known separation in the flexed finger (Garcia-Elias et al., 1991; Zancolli, 1979

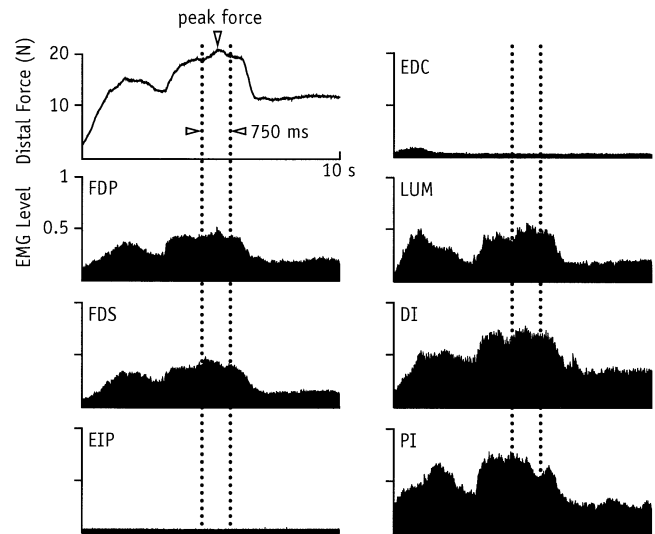


Fig. 2. Representative sample trial (10 s duration) of distal force and fine-wire intramuscular electrode recordings from the seven muscles of the index-finger. Standard approaches were used to record from *extensor indicis proprius* (EIP) and *first dorsal interosseous* (DI) (Delagi et al., 1981). Novel approaches were developed to record from *first lumbrical* (LUM), *first palmar interosseous* (PI) and the index-finger slips of *flexor digitorum profundus*, *flexor digitorum superficialis* and *extensor digitorum communis* (FDP, FDS and EDC, respectively) (Burgar et al., 1997). Only 4 of 56 electrode placements were unsuccessful. We were unable to obtain FDP and FDS signals without cross-talk from middle finger flexor muscles in one subject. Two PI electrodes failed in separate subjects (one deteriorated to a weak signal in mid-experiment; the other had cross talk from the adjacent second dorsal interosseous muscle). EMGs (100 Hz–20 kHz band-pass filtered, amplified, full-wave rectified and smoothed,  $\tau = 20$ ms) recorded in each trial were normalized by the value obtained during separate maximal isometric voluntary contractions of each muscle. These contractions were performed immediately before and after force production while the investigator braced the finger in the standard posture. In each trial, under concurrent visual feedback, subjects sequentially developed moderate, maximal and moderate force. The force and normalized EMG signals were each averaged over 750 ms centered on peak force. The coefficient of variation (S.D./mean) averaged over all directions during production of maximal force was  $2.4 \pm 1.4$  and  $11.2 \pm 1.1\%$  for force and EMG levels, respectively.

Fig. 4B). The DI model inserted into the proximal phalanx exclusively (An et al., 1983; Brand and Hollister, 1993; Ikebuchi et al., 1988; Tubiana, 1981) (Fig. 3B).

Isometric force production by each muscle was modeled by scaling its maximal force  $f_{0i}$  by its excitation level  $e_i$  ( $0 \leq e_i \leq 1$ ) using a generic muscle model (Zajac, 1989). Nominal  $f_{0i}$  values were obtained by multiplying physiological cross-sectional areas (PCSAs) (An et al., 1985, Table 1) times maximal muscle stress ( $35 \text{ N/cm}^2$  (Zajac, 1989)). We assumed muscles were at optimal fiber length due to lack of published values, with pennation angles (Jacobson et al., 1992; Lieber et al., 1992) low enough not to affect  $f_{0i}$  (i.e.  $< 10^\circ$  (Zajac, 1989)).

The computer model is a matrix equation where the static force production properties of the finger are

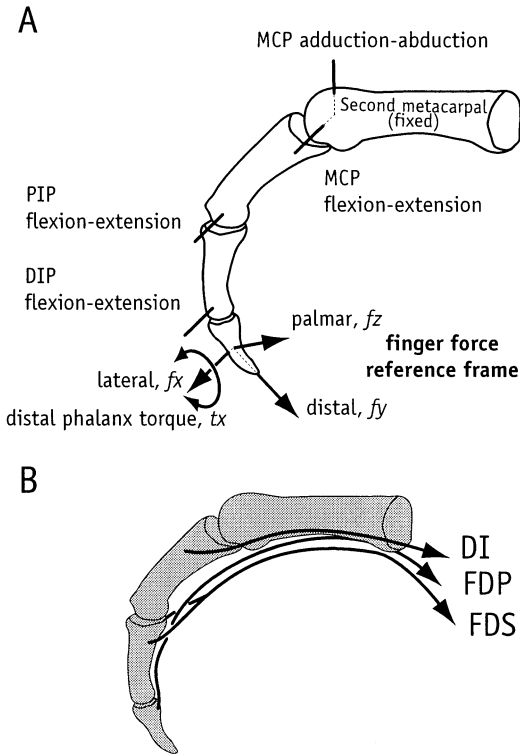


Fig. 3. Index finger model. (A) Four DOFs articulate the fixed metacarpal and three phalanges: two perpendicular hinges (ad-abduction and flexion–extension at the MCP joint (Youm et al., 1978b)) and a single flexion–extension hinge at the PIP and DIP joints (An et al., 1979). The force reference frame fixed to fingertip was oriented with the lateral, distal and palmar forces. Dorsal force is opposite to palmar; medial is opposite to lateral. Because of the presence of three flexion–extension hinges, the distal phalanx can control a torque in the sagittal plane (i.e., ‘distal phalanx torque’) independently of finger force. (B) Tendon paths of the DI, FDP and FDS (see Fig. 4B for other tendon paths).

contained in a  $4 \times 7$  matrix  $\mathbf{M}$  (Eq. (1)) that maps a seven-element input vector  $\mathbf{e}$  (i.e., muscle excitation pattern) into a four-element vector  $\mathbf{ft}$  (i.e., lateral ( $f_x$ ), distal ( $f_y$ ) and palmar ( $f_z$ ) force, and torque at the distal phalanx ( $t_x$ ), Fig. 3A):

$$\mathbf{ft} = \begin{Bmatrix} f_x \\ f_y \\ f_z \\ t_x \end{Bmatrix} = \mathbf{M} \begin{Bmatrix} e_{\text{FDP}} \\ e_{\text{FDS}} \\ e_{\text{EIP}} \\ e_{\text{EDC}} \\ e_{\text{LUM}} \\ e_{\text{DI}} \\ e_{\text{PI}} \end{Bmatrix} = \mathbf{M}\mathbf{e}, \quad (1)$$

$$\mathbf{M} = \mathbf{J}^{-\text{T}}\mathbf{R}\mathbf{F}_0, \quad (2)$$

$\mathbf{M}$  (Eq. (2)) is the concatenation of the  $7 \times 7 \mathbf{F}_0$  diagonal matrix of nominal  $f_{0i}$  values (scales the excitation level of each muscle into muscle force), the  $4 \times 7 \mathbf{R}$  moment arm and extensor mechanism interaction matrix (superimposes

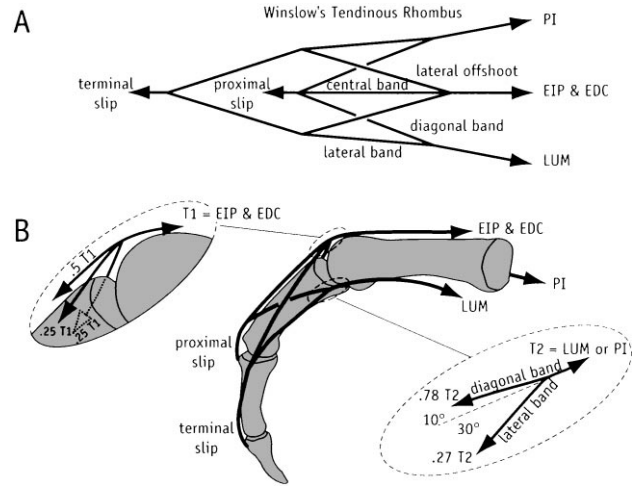


Fig. 4. Extensor mechanism model. A radio-ularly symmetric adaptation of Winslow’s tendonous rhombus (Zancolli, 1979) is used. (A) Tendons from the EIP and EDC, PI and LUM combine to form the proximal and terminal slips, which have extensor moment arms at the interphalangeal joints (Table 1). (B) The central band and each lateral offshoot from EIP and EDC were nominally assumed to receive one-half and one-quarter of the tension ( $T_1$ ) in the combined extensor tendon, respectively (left insert). The bifurcations of LUM and PI tendons ( $T_2$ ) into the diagonal and lateral bands (known to increase with finger posture (Garcia-Elias et al., 1991)) are considered nodes of a flat net in static equilibrium where the tension in each band depends on their relative orientation (right insert). The angles of the diagonal and lateral bands with respect to the proximal tendon were nominally set to 10 and 30°, respectively, and to 79 and 39° in the adjusted model (Table 1). Tensions in the proximal and terminal slips were assumed to be algebraic sums of the tensions in the bands and offshoots.

the joint torque vector produced by each muscle force to obtain the net joint torque vector), and the  $4 \times 4 \mathbf{J}^{-\text{T}}$  inverse transpose Jacobian matrix of the three-phalanx/four-DOF finger (calculates the  $\mathbf{ft}$  produced by the net joint torque vector).  $\mathbf{J}^{-\text{T}}$  implicitly satisfies static equilibrium as the finger will hold its posture if  $\mathbf{ft}$  is resisted (Yoshikawa, 1990). The 35 anatomical parameters of  $\mathbf{M}$  were either obtained from the literature (3 phalanx lengths, 22 moment arm values, and 7 PCSAs) or assumed (3 extensor mechanism parameters due to lack of published material). These parameters were defined as either independent (Table 1), dependent (Table 2) or fixed (Table 2). For a given finger posture and no constraints on  $\mathbf{e}$ ,  $\mathbf{M}$  is a constant non-invertible matrix, i.e., several  $\mathbf{e}$  can produce a given  $\mathbf{ft}$ .

With the bounds on  $e_i$  and the constraint  $t_x = 0$ , the unique  $\mathbf{e}$  producing the maximal biomechanically feasible magnitude of a given  $\mathbf{ft}$  was computed geometrically (Chao and An, 1978; Gordon, 1990; Kuo and Zajac, 1993; Spoor, 1983). A muscle excitation pattern  $\mathbf{e}$  specifies a point in seven-dimensional ‘excitation space’ (i.e., with as many orthogonal axes as there are muscles where the excitation of each muscle is a value on the appropriate axis). Because  $0 \leq e_i \leq 1$ , all achievable  $\mathbf{e}$  lie inside a seven-dimensional cube of sides 1 (i.e., unit hypercube).

Table 1  
Independent model parameters

	Tendon	Nominal Model	Adjusted Model	% Change
<i>Joint</i> (Moment arms, mm (An, et al., 1983))				
MCP adduction	FDP	2.90	—	0
(Adduction +)	EIP	0.30	—	0
(Abduction -)	EDC	-1.19	—	0
	LUM	-3.84	-4.61	+20
	DI	-6.77	—	0
	PI	4.08	6.94	+70
MCP flexion	FDP	12.00	9.00	-25
(Flexion +)	EIP	-7.77	-9.32	+20
(Extension -)	LUM	7.00	—	0
	DI	2.00	—	0
	PI	4.00	—	0
PIP flexion	FDP	6.50	5.07	-22
	proximal slip	-2.75	-3.44	+25
DIP flexion	FDP	3.64	—	0
	Terminal slip	-1.50	—	0
<i>Item</i> (Extensor mechanism)				
Proportion to proximal slip		50%	62.5% + 25	
Top bifurcation angle		10°	79° + 690	
Bottom bifurcation angle		30°	39° + 30	
<b>PCSA</b> , cm <sup>2</sup> (An et al., 1985)				
	Muscle			
	FDP	4.10	—	0
	FDS	3.65	7.30	+100
	EIP	1.12	0.78	-30
	EDC	1.39	3.06	+120
	LUM	0.36	0.72	+100
	DI	4.16	—	0
	PI	1.60	4.32	+170

*Note:* The maximal force an individual muscle could produce,  $f_{0i}$ , was calculated by multiplying PCSA by maximal muscle stress (35 N/cm<sup>2</sup>) (Zajac, 1989). Optimum muscle fiber length was assumed due to the lack of published values, and pennation angles (Jacobson et al., 1992; Lieber et al., 1992) were assumed low enough not to affect  $f_{0i}$  (i.e.,  $< 10^\circ$  (Zajac, 1989)). Adding tendon length and elasticity would add unnecessary redundancy to the calculation of maximal isometric force as optimum muscle fiber length is unknown. The adjusted PCSA values represent, in effect, the lower bound of force needed by each muscle in this finger posture.

The fourth row of  $\mathbf{M}$  specifies how  $\mathbf{e}$  is combined to produce distal phalanx torque,  $t_x$ . Taking this row as a vector and finding its nullspace identifies all excitation patterns that will produce zero distal phalanx torque when mapped through  $\mathbf{M}$ , consistent with the experimental task. Using principles of Computational Geometry (Avis and Fukuda, 1992) we calculated the intersection of this null space with the unit hypercube to find the region of excitation space containing all  $\mathbf{e}$  that produce  $\mathbf{ft}$  with zero distal phalanx torque elements. Finally, mapping the extreme points of this seven-dimensional region through  $\mathbf{M}$  produces a convex polyhedron (Chvátal, 1983) in three-dimensional output Cartesian 'force space' (i.e.,  $\{f_x, f_y, f_z, 0\}^T$ ,  $t_x$  is zero by construction). The surface of this force polyhedron represents the limits

on achievable  $\mathbf{ft}$  vectors with zero distal phalanx torque (Chao and An, 1978; Gordon, 1990; Kuo and Zajac, 1993; Spoor, 1983). Thus, a point on the surface of this three-dimensional polyhedron in force space is produced by a unique excitation pattern, and the distance to the origin specifies the maximal biomechanically achievable magnitude for that static force when  $t_x = 0$ .

An adjusted model was generated by modifying independent parameters of the nominal model, guided by a sensitivity analysis, to better reproduce experimental force magnitudes. The sensitivity of fingertip force to each independent parameter was the predicted change in maximal force magnitude to a 10% perturbation of each parameter. The parameters that affected force predictions most were the first candidates for modification, if

Table 2  
Fixed and dependent model parameters

	Tendon	Fixed	Proportional to	Rationale
<i>Phalanges</i>				
Proximal		50 mm		(An et al., 1979)
Middle		31 mm		(An et al., 1979)
Distal		16 mm		(An et al., 1979)
<i>Joint (Moment arms)</i>				
MCP abduction	FDS		0.5 FDP	(An et al., 1983).
MCP flexion	FDS		1.1 FDP	(An et al., 1983).
	EDC		EIP	(An et al., 1983).
PIP flexion	FDS		0.9 FDP	(An et al., 1983)
	EIP		Proximal slip	Winslow's rhombus (Fig. 4).
	EDC		Proximal slip	Winslow's rhombus (Fig. 4).
	LUM		Proximal slip	Winslow's rhombus (Fig. 4).
	DI	0 mm		No middle phalanx insertion (Tubiana, 1981; An et al., 1983; Ikebuchi et al., 1988).
DIP flexion	PI		Proximal slip	Winslow's rhombus (Fig. 4).
	FDS	0 mm		No distal phalanx insertion (Tubiana, 1981).
	EIP		Terminal slip	Winslow's rhombus (Fig. 4).
	EDC		Terminal slip	Winslow's rhombus (Fig. 4).
	LUM		Terminal slip	Winslow's rhombus (Fig. 4).
	DI	0 mm		No distal phalanx insertion (Tubiana, 1981).
	PI		Terminal slip	Winslow's rhombus (Fig. 4).

such modifications could be anatomically or functionally justified.

### 3. Results

Fingertip forces in all directions were directed accurately (within  $4.7 \pm 2.2^\circ$  (S.D.) of target) and their magnitudes clustered into three distinct levels ( $p < 0.05$ , post hoc pairwise repeated measures ANOVA, Table 3). Palmar, distal and medial forces were comparable and significantly higher than lateral force, which was greater than dorsal force. The coefficient of variation (S.D./mean) of force magnitude averaged over all directions was  $2.4 \pm 1.4\%$ .

Repeated measures analysis of variance found distinct excitation levels for each muscle relative to each force direction were found ( $p < 0.05$ ). In addition, post hoc analyses revealed that dorsal, palmar and distal forces displayed 4, 2 and 3 distinct groups of muscle excitation, respectively ( $p < 0.05$ , summarized as non-overlapping groups in Table 4; see Discussion for LUM in dorsal force). While no distinct groups of muscle excitation were found for lateral and medial force directions (overlapping groups in Table 4), both interossei were excited at an intermediate level for lateral force, and DI and PI were the most and least excited muscles for medial force, respectively. The coefficient of variation of EMG magnitude during maximal force averaged  $11.2 \pm 1.1\%$  over all

Table 3  
Force magnitudes (N)

Direction	Grouping by magnitude ( $p < 0.05$ )	Experimental Mean $\pm$ SD	Predicted	
			Nominal model	Adjusted model
Palmar	a	$27.9 \pm 4.1$	17.3	24.2
Distal	a	$24.3 \pm 8.3$	17.4	38.9
Medial	a	$22.9 \pm 7.8$	15.0	23.7
Lateral	b	$14.7 \pm 4.8$	27.2	32.1
Dorsal	c	$7.5 \pm 1.5$	4.1	6.9

*Note:* Forces with and without EMG electrodes are combined because no significant difference between them exists (Burgar et al., 1997). Average force magnitudes for each direction were statistically grouped into three levels (labeled as a, b and c) by post-hoc pairwise RH ANOVA comparisons. Because the model cannot reproduce interosseous muscle co-excitation for lateral and medial forces, little confidence is placed in the magnitude predictions for these force directions.

directions. The fact that the CV of EMG is greater than that of force is not unexpected given that force can be considered the low-pass filtered version of EMG (Zajac, 1989).

The nominal model qualitatively reproduced extensor activity in all force directions, and PI excitations for dorsal, palmar, distal and medial forces, but underestimated flexor activity for all forces except for medial (Fig. 5). The experimental and predicted patterns of muscle

Table 4  
Statistical grouping of mean EMG levels (% of reference MVC,  $p < 0.05$ )

	Mean	Group
Dorsal force	FDP	D1
	FDS	DA
	DI	DA
	LUM	D1 D2
	PI	D2
	EDC	D3
	EIP	D4
Palmar force	PI	P1
	DI	P2
	FDS	P2
	LUM	P2
	EIP	P2
	EDC	P2
	FDP	P2
Distal force	EIP	I1
	EDC	I1
	FDS	I2
	FDP	I2
	LUM	I2
	DI	I3
	PI	I3
Lateral force	FDS	L1
	FDP	L1 L2
	LUM	L1 L2
	DI	L2 L3
	PI	L3 L4
	EIP	L3 L4
	EDC	L4
Medial force	PI	M1
	EDC	M1
	EIP	M1 M2
	FDP	M1 M2
	FDS	M1 M2
	LUM	M1 M2
	D1	M2

Note: Statistical grouping of muscles by mean normalized EMG level (ANOVA post-hoc pairwise comparisons,  $n = 8$ ,  $p < 0.05$ ). The seven finger muscles are ranked by mean normalized EMG level for each force direction. Post hoc pairwise comparisons were justified because significant ANOVA result were found for all force directions ( $p < 0.05$ ). All significant pairwise differences are summarized as group letters where each mean is shown to belong to a specific group. Clear differentiation among 4, 2 and 3 distinct excitation groups was found for dorsal, palmar and distal forces, respectively (LUM excitation is predicted to affect dorsal force little). While group differentiation was not as clear for lateral and medial forces, both interossei were co-excited for lateral force, and PI and DI were the least and most excited muscles for medial force, respectively ( $p < 0.05$ ). The mean + 3 S.D. of baseline noise level in all EMG channels averaged  $7.9 \pm 4.5\%$ . Mean  $\pm$  S.D. coefficient of variation was  $11.2 \pm 1.1\%$  during maximal force production across all directions. Muscle excitation levels during force production remained below 76% of reference MVC.

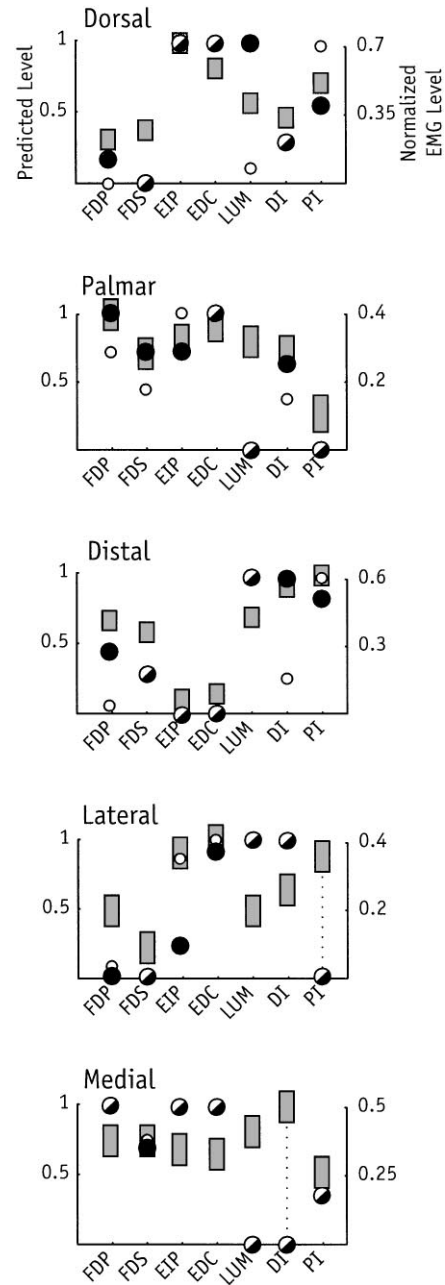


Fig. 5. Qualitative comparison of mean normalized EMG levels (rectangles, mean  $\pm$  S.E., right hand scale) to muscle excitations generated by the nominal (open circles) and adjusted (filled circles) models (left hand scale). Because subjects did not exhibit EMG levels higher than 76% of reference MVCs during force production, the highest EMG value observed in a given force direction (right hand scale) is plotted as equivalent to maximal excitation in the model (1, left hand scale) to facilitate the qualitative comparison of excitation patterns. Six moment arms and five PCSAs (Table 1) were modified, guided by sensitivity analyses, to arrive at the adjusted model. Half-filled circles indicate no change in predicted excitation after adjustments. The excitations of the adjusted model for dorsal, palmar and distal forces compare favorably with the experimental EMGs. Discrepancies in LUM excitations are not considered critical given the low relative strength of this muscle and low sensitivity of force production to its parameters (Table 5). Reasonable modifications to the independent parameters are incapable of producing co-activation of DI and PI in lateral and medial forces (dotted lines); thus confidence in the excitation and force predictions for these two force directions is low.

Table 5  
Relative sensitivity of predicted force magnitudes to independent parameters of adjusted model

	Tendon	Dorsal	Palmar	Distal
<i>Joint (Moment arms, mm)</i>				
MCP adduction	FDP	—	—	– 0.21
	EIP	—	—	—
	EDC	—	—	—
	LUM	—	—	—
	DI	—	—	+ 0.77
	PI	—	—	– 0.67
MCP flexion	FDP	—	– 0.86	<u>0.90</u>
	EIP	—	0.50	—
	LUM	—	—	0.14
	DI	—	—	0.23
	PI	—	—	0.37
PIP flexion	FDP	– 0.24	<u>1.00</u>	– 0.90
	proximal slip	1.00	– 0.23	<u>0.50</u>
DIP flexion	FDP	0.26	0.24	0.18
	terminal slip	– 0.62	—	– 0.17
<i>Item (Extensor mechanism)</i>				
Proportion to proximal slip		0.80	– 0.21	—
Top bifurcation angle		0.40	—	0.50
Bottom bifurcation angle		– 0.39	—	– 0.17
<b>PCSA, cm<sup>2</sup></b>				
	Muscle			
	FDP	—	0.34	—
	FDS	—	—	—
	EIP	—	—	—
	EDC	0.32	0.16	—
	LUM	—	—	0.29
	DI	—	—	1.00
	PI	—	—	—

*Note:* Relative sensitivity of dorsal, palmar and distal force magnitudes to each independent parameter. Columns are normalized by the magnitude of the largest sensitivity for each force direction. Positive values indicate that force magnitude will increase with an increase in absolute value of parameter, ‘—’ indicates relative sensitivity is below 0.10. Because optimal fiber length and rigid tendons are assumed (see Discussion), PCSA is used as an estimate of the minimum *effective* force needed by each muscle in this finger posture. Because the model cannot reproduce interosseous muscle co-excitation for lateral and medial forces, the predicted sensitivities for lateral force may not apply and are not presented.

Note the opposite effects of FDP moment arms on palmar and distal force magnitudes (opposite signs of underlined numbers).

coordination were qualitatively compared by overlaying their plots and showing the highest EMG value of each force direction equivalent to the maximal predicted excitation level of 1. The nominal model underestimated palmar, distal, medial and dorsal force magnitudes by 38, 28, 34 and 45%, respectively, and overestimated lateral force by 2 times (Table 3).

An adjusted model was created by modifying five of seven PCSAs and six of 15 independent moment arms in the nominal model (Table 1). In it, flexor and DI activity for dorsal, palmar and distal forces agreed better with their EMG measurements (Fig. 5). No reasonable adjustments to either model could reproduce interossei co-

excitation for lateral and medial forces (Fig. 5); thus, little confidence is placed in the force and EMG predictions for these forces. The adjusted model replicated well palmar and dorsal forces, and overestimated distal force by 1.6 times.

The difference between predicted and measured LUM excitation during dorsal and palmar forces (Fig. 5) was not critical because of their low sensitivity to LUM parameters (Table 5; see Discussion). A sensitivity analysis of the adjusted model (Table 5) predicts dorsal force to be most sensitive to the moment arm of and the tension allocation to the PIP extensor tendon of the extensor mechanism. Distal force is most sensitive to DI strength.

MCP and PIP flexor moment arms (underlined numbers in Table 5) can have strong and opposite effects on palmar and distal forces.

#### 4. Discussion

Understanding the mechanical significance of subject-independent muscle excitation patterns during the production of maximal voluntary fingertip forces is important for evaluation of surgical options to restore grasping function. Mechanically, it is realistic to expect subject-independent muscle excitation patterns during maximal force production because of the unique coordination strategies (Chao and An, 1978; Gordon, 1990; Kuo and Zajac, 1993; Spoor, 1983) required to produce the maximal magnitude of the net joint torques needed for maximal fingertip forces (Table 6). Clinically, the ability to coordinate transferred tendons (Leffert and Meister, 1976; Moberg, 1990; Waters et al., 1990) suggests it is reasonable to expect the CNS to converge on mechanically advantageous excitation patterns. However, EMG recordings during index-finger force production had not identified subject-independent patterns (Close and Kidd, 1969; Long et al., 1970; Maier and Hepp-Reymond, 1995).

The novel electrode placement technique (Burgar et al., 1997) and the uniform force production task studied enabled us to identify subject-independent ranking of fingertip forces and muscle excitations. By standardizing finger and wrist posture, the variability in the location on the  $f$ -1 curve where the muscle fibers operated was lowered, thereby reducing the variability in force magnitudes (Mathiowetz et al., 1985; O'Driscoll et al., 1992; Weightman and Amis, 1982) and EMG signals (Zajac, 1992). Intramuscular electrodes did not affect force magnitudes (Burgar et al., 1997). The conflicting observations by others of substantial (Close and Kidd, 1969) and zero (Weightman and Amis, 1982) extensor activity during 'tip pinch' may be due to subjects generating palmar force in the former and distal force in the latter study.

Reports of higher finger force magnitudes (An et al., 1985; Weightman and Amis, 1982) and our below-MVC excitation levels (Table 4) suggest maximal forces were

not generated by our subjects. The ball-impregnated thimbles presented subjects with a precarious task, much like pressing a thumb tack into a low-friction impenetrable surface, which may have prevented maximal effort. The limited time allotted to produce force, and the potential thimble loosening due to fingerpad compression during palmar, lateral and medial forces, may have also contributed. For distal force, the possible discomfort of the fingernail against the thimble, together with the particularly precarious tendency of the DIP joint to hyperextend if the force was not precisely directed, may have reduced its magnitude. Thus, the overestimation of distal force by the model (Table 3) is not considered to invalidate the conclusions of this study. Other limitations of this work are that the index-finger was studied and modeled in mechanical isolation (i.e., muscle synergies may be present during coordination of multiple fingers in grasp), our model of the extensor mechanism addresses its force distribution function only (cf. studies of tendon excursion (Storace and Wolf, 1982; Leijnse and Kalker, 1995)). Also, our assumption that the model predicts the minimum effective force produced by individual muscles (see below) may not apply to LUM given its origin on the FDP tendon.

The favorable match between recorded EMG patterns and those predicted by the adjusted model for dorsal, palmar and distal forces suggests the CNS is implementing the predicted mechanically advantageous strategies, and scaling them down to produce less than maximal forces. The adjusted model placed no constraints on muscle excitations other than to scale and superimpose the complex multiarticular torque capability of each muscle to produce the maximal biomechanically possible magnitude of the target net joint torque vector (Table 6). The mechanically advantageous strategies included (Fig. 5) the use of extensors to produce palmar force (to regulate net joint flexion torques) and of intrinsics (MCP flexors but IP joint extensors via the extensor mechanism) to produce dorsal force, and the absence of extensors for distal force (intrinsic cancel the DIP flexion torque of FDP via the extensor mechanism). The seemingly major difference between predicted and measured LUM excitation for dorsal and palmar forces (Fig. 5) is believed to be minor given the insensitivity of these forces to LUM parameters (Table 5), a likely consequence of LUM's very low force (Table 1).

The need to adjust independent parameters in the nominal model was not unexpected given that these were compiled from different sources (Table 1). Small ( $\leq 25\%$ ) moment arm adjustments are reasonable given the anatomical complexity of the finger tendinous system. The constant-tension method (An et al., 1983) may have underestimated PI adduction moment arm because it inserts into the sides of the extensor mechanism and may be tension dependent. Implementing the lateral portion of the extensor mechanism as an idealized floating net

Table 6  
Normalized net joint torques necessary for fingertip forces

	Direction				
	Dorsal	Palmar	Distal	Lateral	Medial
Joint torques					
MCP adduction	0	0	0	-1	1
MCP flexion	-1	1	1	0	0
PIP flexion	-0.62	0.62	0.11	0	0
DIP Flexion	-0.21	0.21	0	0	0

was critical to reproduce the experimental magnitude of dorsal force (Table 3), and increase the excitation of flexors during dorsal and distal force generation (Fig. 5).

Increasing PCSAs was justified by the large variability in their reported values (An et al., 1985; Jacobson et al., 1992; Lieber et al., 1992) and the fact that they often come from older, sometimes emaciated, cadavers (An, 1996). Even though the adjusted model quantitatively predicted dorsal and palmar force magnitudes, and reasonably approximated distal force magnitude, PCSAs are still likely to be underestimated as subjects generated the force magnitudes predicted by the model with excitations below 100% MVC. Increasing PCSAs equally would cause better force predictions.

Our adjusted PCSA values represent the lower bound of force needed by each muscle in this finger posture. The maximal force of a muscle at a given length depends on the combined effects of tendon resting length, tendon compliance and muscle fiber length, among others. Measurements of these tendon and muscle fiber parameters are unavailable for index-finger muscles, and including these parameters would introduce unnecessary redundancy in our model. By assuming muscles to lie at optimal fiber length and to have inextensible tendons, PCSA becomes, in effect, an estimate of the minimum effective force of each muscle at this posture. Our reduction of EIP PCSA (Table 1), however, does not necessarily mean that its value is incorrect, as EIP may simply be far from optimal fiber length at this posture. We did not change the well-documented value of maximal muscle stress (Zajac, 1989).

Interossei co-contraction may be evidence of a strategy to protect the ligamentous structures of the MCP (Long, 1970) from the torsion induced by medial-lateral forces (Fig. 5). In our models, because torsion is passively resisted by idealized pin-joints, interossei co-contraction is not predicted; otherwise the net ad-abduction torques and the medial-lateral force magnitudes would have been smaller. Thus, interossei co-contraction may be a strategy to prevent strain in the complex ligamentous structures (Youm et al., 1978a) providing MCP joint torsional integrity.

The sensitivity analysis of the adjusted model identified the relatively few biomechanical parameters most affecting force magnitudes (Table 5). The strength of a muscle naturally bounds the magnitude of the joint torque vector it produces and, indeed, distal force is most sensitive to DI PCSA. Moment arms also bound the joint torque vector, and distal and palmar forces are very sensitive to MCP and PIP flexor moment arms (underlined numbers in Table 5), though each moment arm affects distal and palmar force oppositely. Thus, even though both forces require net flexion torques (Table 6), increasing flexor moment arms at the MCP and PIP joints reduces and enhances palmar force, respectively, and vice versa for distal force. The reason is that muscles

need to be coordinated to produce the desired net joint torque at each joint simultaneously. However, each joint torque cannot be controlled individually as muscles simultaneously produce torques at all joints spanned. Because palmar and distal forces require net flexion torque at the MCP and PIP joints (Table 6), extrinsic flexors are necessary to generate these forces. The ratios of MCP:PIP moment arms for FDP and FDS are 1:0.54 and 1:0.44, respectively (from Tables 1 and 2). These moment arm ratios are lower than the net joint torque ratio of 1:0.65 necessary for palmar force, and higher than the net joint torque ratio of 1:0.11 necessary for distal force (Table 6). Increasing FDP and FDS moment arms at the MCP moves the ratios of MCP:PIP further from the desired ratio for palmar force, and closer to that for distal force. Thus, the predicted maximal magnitude of palmar force is reduced and that for distal force increased. The opposite effect is seen when FDP and FDS moment arms are increased at the PIP (Table 5). Dorsal force is most sensitive to the moment arm of and tension allocation to the PIP extensor tendon of the extensor mechanism.

## Acknowledgements

The authors wish to express their deep gratitude to Dr Kai-Nan An for providing a complete set of moment arm data, inviting Dr. Valero-Cuevas to his laboratory to implement the first prototype of our force measurement technique, and advising us on EMG recording protocol; and Dr Vincent R. Hentz for his insightful guidance into the clinical and biomechanical aspects of finger function. We also wish to thank Dr H.F. Machiel Van der Loos and Dr Peter Lum for their help in implementing the experimental apparatus, Dr. Kevin C. McGill for his assistance with data collection, and M. Elise Johanson MS, PT for placing the electrodes in four subjects. Dr Richard Lieber and Dr Kelly Cole provided helpful insights on the anatomy and function of the index finger.

This work was supported by the Rehabilitation R and D Service of the Department of Veterans Affairs (VA) and NIH grant NS17662.

## References

- An, K.N., 1996. Personal communication.
- An, K.N., Chao, E.Y., Cooney, W.P., Linscheid, R.L., 1979. Normative model of human hand for biomechanical analysis. *Journal of Biomechanics* 12, 775–788.
- An, K.N., Chao, E.Y., Cooney, W.P., Linscheid, R.L., 1985. Forces in the normal and abnormal hand. *Journal of Orthopaedic Research* 3, 202–211.
- An, K.N., Ueba, Y., Chao, W.P., Cooney, E.Y., Linscheid, R.L., 1983. Tendon excursion and moment arm of index finger muscles. *Journal of Biomechanics* 16, 419–425.

- Avis, D., Fukuda, K., 1992. A pivoting algorithm for convex hulls and vertex enumeration of arrangements and polyhedra. *Discrete and Computational Geometry* 295–313.
- Brand, P., Hollister, A., 1993. *Clinical Mechanics of the Hand*, 2nd Edn. Mosby-Year Book, Inc, St. Louis.
- Burgar, C.G., Valero-Cuevas, F.J., Hentz, V.R., 1997. Improving selectivity of fine-wire electrode placement for kinesiological and clinical studies: Application to index finger musculature. *American Journal of Physics Medical Rehabilitation* 76, 1–9.
- Chao, E.Y., An, K.N., 1978. Graphical interpretation of the solution to the redundant problem in biomechanics. *Journal of Biomechanical Engineering* 100, 159–167.
- Chvátal, V., 1983. *Linear Programming*. W.H. Freeman and Company, New York.
- Close, J.R., Kidd, C.C., 1969. The functions of the muscles of the thumb, the index, and long fingers. Synchronous recording of motions and action potentials of muscles. *Journal of Bone and Joint Surgery (American)* 51, 1601–1620.
- Delagi, E.F., Perotto, A., Thomas, H., 1981. *Anatomic Guide for the Electromyographer—the Limbs*, 2nd Edn. Charles C. Thomas, Springfield.
- Delp, S., Maloney, W., 1993. Effects of hip center location on the moment-generating capacity of the muscles. *Journal of biomechanics* 26, 485–499.
- Enoka, R.M., Stuart, D.G., 1992. Neurobiology of muscle fatigue. *Journal of Applied Physiology* 1631–1648.
- García-Elias, M., An, K.N., Berglund, L., Linscheid, R.L., Cooney, W.P., Chao, E.Y., 1991. Extensor mechanism of the fingers: I. A quantitative geometric study. *Journal of Hand Surgery (American)* 16, 1130–1140.
- Gordon, M.E., 1990. An analysis of the biomechanics and muscular synergies of human standing, PhD Thesis, Stanford University, Stanford.
- Graves, J.E., James, R.J., 1990. Concurrent augmented feedback and isometric force generation during familiar and unfamiliar muscle movements. *Research Quarterly for Exercise Sport* 61, 75–79.
- Harding, D.C., Brandt, K.D., Hillberry, B.M., 1993. Finger joint force minimization in pianists using optimization techniques. *Journal of Biomechanics* 26, 1403–1412.
- Hentz, V.R., Hamlin, C., Keoshian, L.A., 1988. Surgical reconstruction in tetraplegia. *Hand Clinics* 4, 601–607.
- Hentz, V.R., House, J., McDowell, C., Moberg, E., 1992. Rehabilitation and surgical reconstruction of the upper limb in tetraplegia: an update. *Journal of Hand Surgery (American)* 17, 964–967.
- Ikebuchi, Y., Murakami, T., Ohtsuka, A., 1988. The interosseous and lumbrical muscles in the human hand, with special reference to the insertions of the interosseous muscles. *Acta Medica Okayama* 42, 327–334.
- Jacobson, M.D., Raab, R., Fazeli, B.M., Abrams, R.A., Botte, M.J., Lieber, R.L., 1992. Architectural design of the human intrinsic hand muscles. *Journal of Hand Surgery (American)* 17, 804–809.
- Kelsey, J.L., 1984. Prevalence studies of the epidemiology of osteoarthritis. In: Lawrence, R.C., Shulman, L.E. (Eds.), *Epidemiology of the Rheumatic Disease*, Chap. 39., Gower Medical Publishing, Ltd, New York, pp. 282–288.
- Krishnan, J., Chipchase, L., 1997. Passive axial rotation of the metacarpophalangeal joint. *Journal of Hand Surgery (B)* 22B(2), 270–273.
- Kuo, A.D., Zajac, F.E., 1993. A biomechanical analysis of muscle strength as a limiting factor in standing posture. *Journal of Biomechanics* 26 (Suppl 1), 137–150.
- Lee, J.W., Rim, K., 1990. Maximum finger force prediction using a planar simulation of the middle finger. *Proceedings of the Institution of Mechanical Engineers Part H, Journal of Engineering in Medicine* 204, 169–178.
- Leffert, R.D., Meister, M., 1976. Patterns of neuromuscular activity following tendon transfer in the upper limb: a preliminary study. *Journal of Hand Surgery (American)* 1, 181–189.
- Leijnse, J.N., Kalker, J.J., 1995. A two-dimensional kinematic model of the lumbrical in the human finger. *Journal of biomechanics* 28, 237–249.
- Lieber, R.L., Jacobson, M.D., Fazeli, B.M., Abrams, R.A., Botte, M.J., 1992. Architecture of selected muscles of the forearm: anatomy and implications for tendon transfer. *Journal of Hand Surgery (American)* 17, 787–798.
- Long, C., Conrad, P.W., Hall, E.A., Furler, S.L., 1970. Intrinsic-extrinsic muscle control of the hand in power grip and precision handling. An electromyographic study. *Journal of Bone and Joint Surgery (American)* 52, 853–867.
- Maier, M.A., Hepp-Reymond, M.C., 1995. EMG activation patterns during force production in precision grip. I. Contribution of 15 finger muscles to isometric force. *Experimental Brain Research* 103, 108–122.
- Mathiowetz, V., Kashman, N., Volland, G., Weber, K., Dowe, M., Rogers, S., 1985. Grip and pinch strength: normative data for adults. *Archives Physica Medical Rehabilitation* 66, 69–74.
- McFarlane, R.M., 1987. In: McFarlane, R.M. (Ed.), Churchill Livingstone, New York.
- Moberg, E., 1990. Surgery for the spastic, stroke and tetraplegic hand. In: McCarthy, J., (Ed.), *Plastic Surgery* vol. 8, Part 2, (1st edn), W.B. Saunders Company, Philadelphia, pp. 4977–4990.
- Murray, R.M., Li, Z., Sastry, S.S., 1994. *A Mathematical Introduction to robotic manipulation*. CRC Press, Boca Raton, FL.
- O'Driscoll, S. W., Horii, E., Ness, R., Cahalan, T.D., Richards, R.R., An, K.N., 1992. The relationship between wrist position, grasp size, and grip strength. *Journal of Hand Surgery (American)* 17, 169–177.
- Spoor, C.W., 1983. Balancing a force on the fingertip of a two dimensional finger model without intrinsic muscles. *Journal of Biomechanics* 16, 497–504.
- Storage, A., Wolf, B., 1982. Kinematic analysis of the role of the finger tendons. *Journal of Biomechanics* 15, 391–393.
- Thompson, D.E., Buford, W.L., Myers, L.M., Giurintano, D.J., Brewer, J.A., 1988. A hand biomechanics workstation. *Computer Graphics* 22, 335–343.
- Tubiana, R., 1981. In: Tubiana, R. (Ed.), *The Hand*. Saunders, Philadelphia.
- Valero-Cuevas, F.J., 1997. Muscle coordination of the human index finger. Ph.D. Thesis, Stanford University, Stanford.
- Waters, R.L., Stark, L.Z., Gubernick, I., Bellman, H., Barnes, G., 1990. Electromyographic analysis of brachioradialis to flexor pollicis longus tendon transfer in quadriplegia. *Journal of Hand Surgery (American)* 15, 335–339.
- Weightman, B., Amis, A., 1982. Finger joint force predictions related to design of joint replacements. *Journal of Biomedical Engineering* 4, 197–205.
- Yoshikawa, T., 1990. *Foundations of Robotics: Analysis and Control*. The MIT Press, Cambridge, MA.
- Youm, Y., Gillespie, T.E., Flatt, A.E., Sprague, B.L., 1978a. Kinematic investigation of normal MCP joint. *Journal of Biomechanics* 11, 109–118.
- Youm, Y., McMurtry, R.Y., Flatt, A.E., Sprague, B.L., 1978b. Kinematics of the wrist — I. An experimental study of radial-ulnar deviation and flexion-extension. *Journal of Bone and Joint Surgery* A60, 423–431.
- Zajac, F.E., 1989. Muscle and tendon: properties, models, scaling, and application to biomechanics and motor control. *Critical Reviews Biomedical Engineering* 17, 359–411.
- Zajac, F.E., 1992. How musculotendon architecture and joint geometry affect the capacity of muscles to move and exert force on objects: a review with application to arm and forearm tendon transfer design. *Journal of Hand Surgery (American)* 17, 799–804.
- Zancolli, E., 1979. *Structural and Dynamic Bases of Hand Surgery*, 2nd ed. Lippincott, Philadelphia.